Disambiguation of complex subvoxel fibre configurations in high angular resolution fibre tractography

P. Savadjiev[1], J. Campbell[2], M. Descoteaux[3], R. Deriche[3], G. B. Pike[2], and K. Siddiqi[1]

[1]School of Computer Science and Centre for Intelligent Machines, McGill University, Montreal, QC, Canada, [2]McConnell Brain Imaging Centre, McGill University, Montreal, QC, Canada, [3]Groupe Odyssée, INRIA Sophia Antipolis, Sophia-Antipolis, France

Introduction Although high angular resolution diffusion (HARD) MRI can be used to achieve a better precision in fibre tractography than the diffusion tensor model [1], HARD can still result in ambiguous orientation distribution functions (ODFs) in the presence of complex subvoxel fibre configurations and thus confound fibre tracking algorithms. Different fibre geometries can have similar ODFs, but require different actions to be taken in tractography. For example, in the cases of curved and fanning fibres, the ODF will have one broad maximum. For the former, one curve needs to be propagated, whereas for the latter, multiple curves should be followed when propagating in one direction (denoted by a *polarity* vector), but only one when propagating in the other. In this work we apply the 3D curve inference algorithm, described in [2], in a labeling scheme that disambiguates ODFs that result from (1) single fibres (possibly with subvoxel curvature), (2) subvoxel fanning and (3) crossing configurations. The labeling will allow these cases to be treated properly in tractography and thus reduce the occurrence of false positive and false negative connections [1]. For example, the identification of fibre fanning should help to reconstruct the entire cortical-spinal tract as it fans out to the motor cortex, a situation that currently confounds algorithms using only the ODF maxima. In addition to the identification of such voxels, 3D curve inference also infers the polarity of subvoxel fanning. The 3D curve inference method integrates information over a local neighborhood and thus allows for the resolution of ambiguities that cannot be solved by considering only individual ODF shapes [3]. We provide labeling results and the recovery of fanning polarity on synthetic data as well as *in-vivo* human brain data, and show preliminary results that demonstrate a substantial improvement in the performance of a fibre tracking algorithm.

Methods MRI data were acquired on a Siemens 3T Trio MR scanner (Siemens Medical Systems, Erlangen, Germany) using an 8-channel phased-array head coil. Diffusion encoding was achieved using a single-shot spin-echo echo planar sequence with twice-refocused balanced gradients. A dataset designed for q-ball (QB) reconstruction [4] was acquired with 99 diffusion encoding directions, 2mm isotropic voxel size, 63 slices and b=3000 s/mm^2 (q=0.35 μm^{-1}). A 1mm isotropic resolution T1 weighted anatomical scan was also acquired (TR=9.7ms, TE=4ms,α=12^o). The diffusion ODF, Ψ, given by $\Psi(\theta,\phi)=\int_r P(r,\theta,\phi)dr$, with P the diffusion probability density function, was calculated using QB reconstruction and was normalized to unit volume. Additionally, a synthetic HARD dataset was created using the multitensor model for the diffusion ODF [5], with tensor eigenvalues [1700, 300, 300] x 10^{-6} mm^2/s, b=3000 s/mm^2 and a signal-to-noise ratio of 35. The dataset was specifically created to simulate fibre crossings at various angles, as well as subvoxel fibre fanning.

The 3D curve inference method was run as described in [2]. The algorithm models white matter fibres as 3D curves, and infers helical arcs as local approximations to arbitrary 3D curves based on a support measure defined over a local neighborhood. Originally, 3D curve inference was used for diffusion ODF regularization [2]. In the current work, we introduce a labeling scheme based on the analysis of local configurations of these helical curve approximations. The key idea is to regard regularized ODF maxima as tangents to underlying fibre orientations [6]. The orientation of each ODF maximum and its associated helical curve approximation, computed through a search of *co-helical* configurations [2] of ODF maxima at other voxels in a local neighborhood, are stored. Voxels with curves that coincide on one side of the voxel and diverge on the opposite side are labeled as fanning. Voxels with crossing curves are labeled as crossings, and voxels with a (possibly curving) single curve are labeled as single fibre voxels. Finally, background voxels and voxels in which the determination of the configuration was not conclusive are not labeled. Streamline fibre tractography was initiated in all voxels in a small ROI in the corpus callosum. For tracking without labeling, the maximum closest to the incoming propagation direction was chosen for streamline propagation. For tracking with labeling, the maximum closest to the incoming propagation direction was chosen in voxels labeled as single curve or crossing. For fanning, all directions within the fan were followed when the polarity indicated fanning, while the merge direction was followed in the merge case. For all directions followed, the direction of propagation was selected from within the cone of uncertainty, determined by the finite angular resolution of the acquisition, for the direction. This was done using a Monte Carlo interative process with 1000 iterations from each start voxel, and streamlines were initiated on a 3x3x3 grid within each start voxel. A connectivity profile of all voxels reached by the propagated streamlines was stored.

Results Inferred helical curves are shown overlaid on the brain ODF (left), in a coronal region of partial volume averaging between the corpus callosum and the cortico-spinal tract. Blue: crossings. Red: single curves. Green: fanning, in which case the two green curves delimit the extent of the fan and are oriented in the direction of the fanning polarity. The same is shown (centre) for the synthetic dataset. Fibre tracking results without (top right) and with (bottom right) the use of labeling information to direct a streamline tracking algorithm are shown in the same region as in (left). In both cases, a small seed (green) is placed in the corpus callosum. All voxels connected to it are shown in red, and the anatomical image is shown in a coronal and in a sagittal plane. The use of the labeling information allowed the recovery of a much wider extent of the fanning of the callosal fibres toward the cortex.

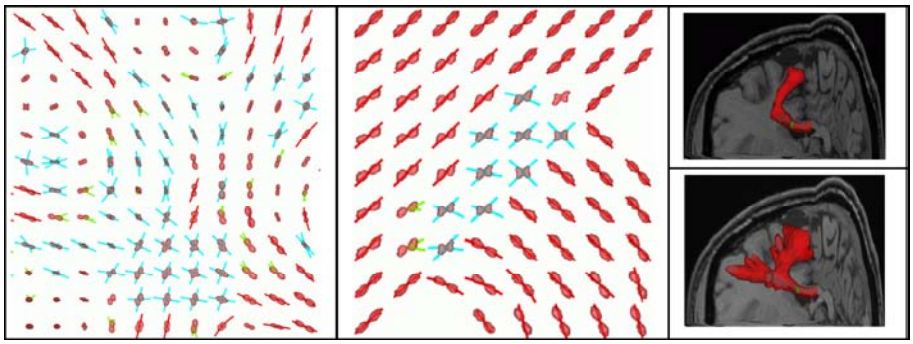

Discussion The results show a successful recovery in both the *in-vivo* and the synthetic datasets of crossing, fanning and single curve configurations in voxels where they are expected to occur. Furthermore, the direction of the polarity in the fanning configurations is correctly recovered. Although no ground truth is available in the brain data, the labeling result and the inferred fibre configurations are anatomically plausible. It can also be seen that the incorporation of the labeling information in the tracking algorithm results in a substantial performance improvement in the *in-vivo* dataset. Currently, the labeling methodology does not distinguish between fanning and smooth branching configurations due to limitations in spatial and angular resolution, and assumes that branching configurations occur significantly less often than fanning configurations. Furthermore, it does not currently deal with bottleneck fibre configurations, as these are not subvoxel configurations but rather occur on a larger scale. Locally, they are indistinguishable from fannings, however, they still require a separate action to be taken in tractography. Contrary to the fanning, bottlenecks require the tracking algorithm to follow only one path, the one with a curvature consistent with the incoming path. These additional configurations will be considered in future work.

References [1] Campbell *et al*. NeuroImage 27(4):725-736, 2005. [2] Savadjiev *et al*. Medical Image Analysis 10(5):799-813,2006. [3] Parker *et al*. Phil.Trans.R.Soc.B 360:893-902,2005. [4] Tuch, D.S. *et al*. Neuron 40(5):885-895, 2003. [5] Descoteaux *et al.* MRM 56:395-410, 2006. [6] Lin *et al*. ISMRM02:442, 2002.